ELSEVIER

Geometric and elastic error calibration of a high accuracy patient positioning system

Marco A. Meggiolaro [a,*], Steven Dubowsky [b], Constantinos Mavroidis [c]

[a] *Department de Engenharia Mecânica, Pontifical Catholic University of Rio de Janeiro, Rua Marquês de São Vicente, 225, Rio de Janeiro, RJ 22453-900, Brazil*
[b] *Department of Mechanical Engineering, Massachusetts Institute of Technology, 77 Massachusetts Avenue, Cambridge, MA 02139, USA*
[c] *Department of Mechanical and Aerospace Engineering, Rutgers University, 98 Brett Road, Piscataway, NJ 08854, USA*

Abstract

Important robotic tasks could be effectively performed by powerful and accurate manipulators. However, high accuracy is generally difficult to obtain in large manipulators capable of producing high forces due to system elastic and geometric distortions. In this work, a high-accuracy patient positioning system is calibrated, consisting of a six degree of freedom manipulator used to position cancer patients during proton therapy sessions. It is found that the original manipulator does not meet the required absolute accuracy due to both geometric and elastic deformation positioning errors. The experimentally identified errors are used to predict, and compensate for, end-point errors as a function of configuration and measured forces, improving the system absolute accuracy. Experimental results show that the adopted methodology is able to effectively correct for the system errors.
© 2004 Elsevier Ltd. All rights reserved.

---

* Corresponding author. Tel.: +55 21 3114 1638; fax: +55 21 3114 1165.
E-mail address: meggi@alum.mit.edu (M.A. Meggiolaro).

1. Introduction

Large robot manipulators are needed in field, service and medical applications to perform high accuracy tasks. Examples are manipulators that perform decontamination tasks in nuclear sites, space manipulators such as the special purpose dexterous manipulator and manipulators for medical treatment [1–3]. In these applications, a large robotic system is often needed to have very fine precision. Its accuracy specifications may be very small fractions of its size. Achieving such high accuracy is difficult because of the manipulator's size and its need to carry heavy payloads. Further, many tasks, such as space applications, require systems to be lightweight, and thus structural deformation errors can be large.

In such systems, two principal error sources create significant end-effector errors. The first is kinematic errors due to the non-ideal geometry of the links and joints of manipulators, such as errors due to machining tolerances. These errors are often called geometric errors. Task constraints often make it impossible to use direct end-point sensing in a closed-loop control scheme to compensate for these errors. Therefore, there is a need for model-based error identification and compensation techniques, often called robot calibration.

The second error source that can limit the absolute accuracy of a large manipulator is the elastic errors due to the distortion of a manipulator's mechanical components under large task loads or even its own weight. Classical error compensation methods do not correct the errors in large systems with significant elastic deformations, because they do not explicitly consider the effects of task forces and structural compliance. Methods have been developed to deal with this problem [4,5], based on analytical models of the manipulator structural properties.

Considerable research has been performed in robot calibration [6–9]. In these methods, robot position accuracy is improved using compensation methods that essentially identify a more accurate functional relationship between the joint transducer readings and the workspace position of the end-effector based on experimental calibration measurements. A major component of this process is the development of manipulator error models, some of which consider the effects of manipulator joint errors, while others focus on the effects of link dimensional errors [10–13]. Error models have been developed specifically for use in the calibration of manipulators [14,15]. Some researchers have studied methods to find the optimal configurations during the calibration measurements to reduce the manipulator errors by calibration [9,16]. Solution methods for the identification of the manipulator's unknown parameters have been studied for these model-based calibration processes [17,18]. Most calibration methods have been applied to industrial or laboratory robots, achieving good accuracy when geometric errors are dominant.

Classical calibration methods do not explicitly compensate for elastic errors due to the wrench at the end-effector. While conceptually very similar to the classical geometric problem, the combined problem is far more complex. Compensating for geometric errors requires building a model that is a function of the n (usually six) joint variables. To compensate for a general six variable end-point task wrench (three end-point forces and three end-point moments) requires a model that is a function of both the joint variables and the end-point wrench variables, or a function of at least 12 variables. The time and cost of the physical calibration measurements often dominates the calibration problem. Simple calculations suggest that a brute force identification would require several million calibration measurements.

In this work, a calibration method is applied to an important medical application of large manipulator systems. The manipulator is used as a high accuracy robotic patient positioning system (PPS) in a proton therapy research facility constructed at the Massachusetts General Hospital (MGH), the Northeast Proton Therapy Center (NPTC) [2,19]. The robotic PPS places a patient in a high energy proton beam delivered from a proton nozzle carried by a rotating gantry structure (see Fig. 1). The PPS is a six degree of freedom manipulator that covers a large workspace of more than 4 m in radius while carrying patients weighing as much as 300 lbs (see Fig. 2). Patients are immobilized on a "couch" attached to the PPS end-effector. The PPS, combined with the rotating gantry that carries the proton beam, enables the beam to enter the patient from any direction, while avoiding the gantry structure. Hence flexibility offered by robotic technology is needed.

The required absolute positioning accuracy of the PPS is ±0.5 mm. This accuracy is critical as larger errors may be dangerous to the patient [20]. The required accuracy is roughly 10^{-4} of the nominal dimension of system workspace, which is a greater relative accuracy than most industrial manipulators. In addition, FEM studies and experimental results show that with a changing payload (between 1 and 300 pounds) and changing configuration the end-effector errors due to elastic deformations and geometric errors are of the order of 6–8 mm. Hence the accuracy is 12–16 times the system specification [21]. However, since the repeatability error of the PPS, defined here as how well the system returns to certain arbitrary configurations, is less than 0.15 mm, it is a good candidate for a model based error correction method.

A calibration method is applied to the PPS with a force/torque sensor built into the system to measure the wrench applied by the patient's weight. The method is able to compensate for the position and orientation errors caused by both geometric and elastic errors. The method explicitly considers the task load dependency of the errors, modeling both deformation and more classical geometric errors in a unified and simplified manner. A set of experimentally measured positions and orientations of the robot end-effector and measurements of the payload wrench are used to
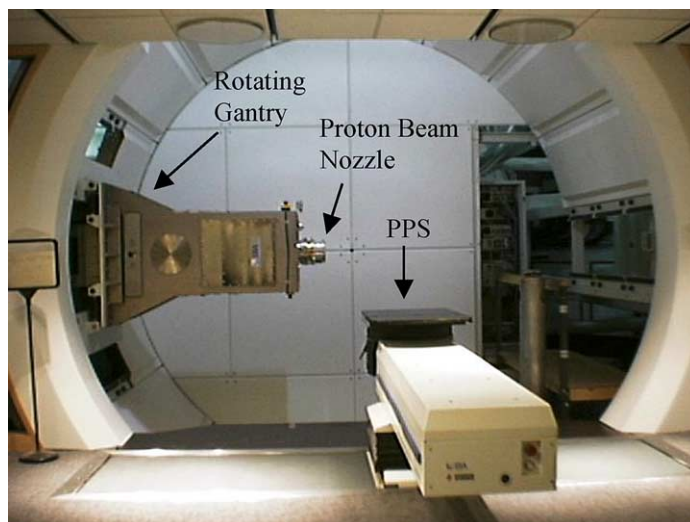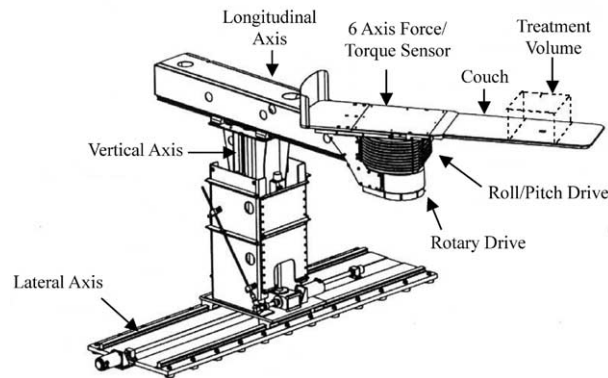

Fig. 1. The PPS and the Gantry.

Fig. 2. The patient positioning system.

calculate the robot errors at each link. It is found that, using only 450 calibration measurements, the end-point errors could be reduced to well within the required specification. In fact, experimental results show that the maximum error was reduced by a factor of 18.

2. Analytical background

There are many possible sources of errors in a manipulator. Mechanical system errors result from machining and assembly tolerances of the manipulator's mechanical components. Joint errors include bearing run-out in rotating joints, rail curvature in linear joints, and backlash in manipulator joints and actuator transmissions. Elastic deformation of the manipulator's members under task loads and gravity can also result in large end-effector errors, especially in long reach manipulator systems. Measurement, actuator, and control errors resulting from the control system also results in end-effector positioning errors. The resolution of encoders and stepper motors are examples of this type of error.

Further, errors can be distinguished into "repeatable" and "random" [22]. Repeatable errors are those with constant numerical value and sign for a given manipulator configuration and task load, such as an assembly error. Random errors are errors that change unpredictably, such as the ones due to backlash of an actuator gear train, when the gear train torque is nearly zero. Classical kinematic calibration and correction can only deal with repeatable errors. It will be shown experimentally in Section 4 that repeatable errors dominate in the performance of the PPS.

To describe the kinematics of a manipulator, Denavit and Hartenberg (DH) reference frames are defined at the manipulator base, end-effector, and at each of the manipulator joints [23]. The position and orientation of a reference frame F_i with respect to the previous reference frame F_{i-1} is defined with DH's 4×4 matrix $\mathbf{A}_i$.

However, system errors cause the geometric parameters of a manipulator to be different from their ideal values. As a result, the frames defined at the manipulator joints are slightly displaced from their expected, ideal locations. The actual position and orientation of a frame F_i^{real} with respect to its ideal location F_i^{ideal} is represented by a 4×4 homogeneous matrix $\mathbf{E}_i$, which character-

izes the standard perturbation of relative link transformation in the serial chain of the mechanism, see Fig. 3. The translational part of matrix $\mathbf{E}_i$ is composed of the three coordinates $\varepsilon_{x,i}$, $\varepsilon_{y,i}$ and $\varepsilon_{z,i}$ of the origin O_i^{real} in F_i^{ideal} (along the X, Y and Z axes respectively, defined using the Denavit–Hartenberg representation), see Fig. 4. The rotational part of matrix $\mathbf{E}_i$ is the result of the product of three consecutive rotations $\varepsilon_{s,i}$, $\varepsilon_{r,i}$, $\varepsilon_{p,i}$ around the Y, Z and X axes respectively (also shown in Fig. 4). These are the Euler angles of F_i^{real} with respect to F_i^{ideal}. The subscripts s, r, and p represent spin (yaw), roll, and pitch, respectively. The six parameters $\varepsilon_{x,i}$, $\varepsilon_{y,i}$, $\varepsilon_{z,i}$, $\varepsilon_{s,i}$, $\varepsilon_{r,i}$ and $\varepsilon_{p,i}$ are called generalized error parameters, which can be a function of the system geometry and joint variables. For an n degree of freedom manipulator, there are $6(n + 1)$ generalized errors which can be written in the form of a $6(n + 1) \times 1$ vector $\varepsilon = [\varepsilon_{x,0}, \ldots, \varepsilon_{x,i}, \varepsilon_{y,i}, \varepsilon_{z,i}, \varepsilon_{s,i}, \varepsilon_{r,i}, \varepsilon_{p,i}, \ldots, \varepsilon_{p,n}]$, with i ranging from 0 to n, assuming that both the manipulator and the location of its base are being calibrated. If the manipulator is being calibrated with respect to its own base, then the error matrix $\mathbf{E_0}$ (which models the base location errors) is eliminated, reducing the number of generalized errors to $6n$. The generalized errors that depend on the system geometry, the system task loads and the system joint variables can be calculated from the physical errors link by link. Note that actual system weight effects can be included in the model as a simple function of joint variables.

When generalized errors are considered, the manipulator loop closure equation takes the form:

$$\mathbf{A_{LC}}(\mathbf{q}, \varepsilon, \mathbf{s}) = \mathbf{E_0}\mathbf{A_1}\mathbf{E_1}\mathbf{A_2}\mathbf{E_2}\cdots\mathbf{A_n}\mathbf{E_n} \tag{1}$$
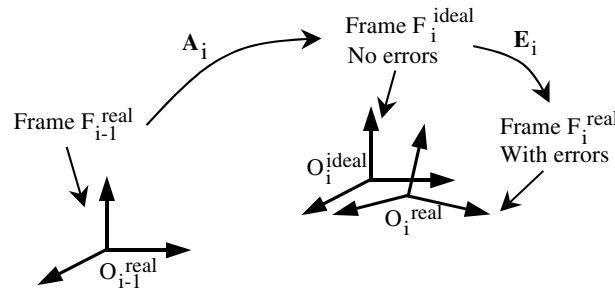

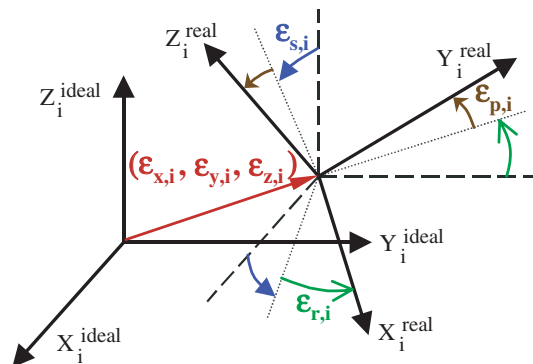Fig. 3. Frame translation and rotation due to errors for ith link.

Fig. 4. Definition of the translational and rotational generalized errors for ith link.

where $\mathbf{A_{LC}}$ is a 4×4 homogeneous matrix that describes the position and orientation of the end-effector frame with respect to the inertial reference frame as a function of the configuration parameters $\mathbf{q}$, the vector of the generalized errors ε, and a vector containing the structural parameters $\mathbf{s}$. The translational components of the matrix $\mathbf{A_{LC}}$ and the three angles of its rotational components are the six coordinates of the end-effector position and orientation vector $\mathbf{X^{real}}$.

The end-effector position and orientation error $\Delta\mathbf{X}$ can be defined as the 6×1 vector that represents the difference between the real position and orientation of the end-effector and the ideal one:

$$\Delta\mathbf{X} = \mathbf{X^{real}} - \mathbf{X^{ideal}} \tag{2}$$

where $\mathbf{X^{real}}$ and $\mathbf{X^{ideal}}$ are the 6×1 vectors composed of the three positions and three orientations of the end-effector reference frame in the inertial reference system for the real and ideal cases, respectively. Since the generalized errors are small, Eq. (2) can be linearized, resulting in an end-effector error represented by the following linear equation in ε:

$$\Delta\mathbf{X} = \mathbf{J_e}\varepsilon \tag{3}$$

where $\mathbf{J_e}$ is the $6 \times 6(n+1)$ Jacobian matrix of the end-effector error $\Delta\mathbf{X}$ with respect to the elements of the generalized error vector ε, also known as Identification Jacobian matrix [24]. As with the generalized errors, $\mathbf{J_e}$ depends on the system configuration, geometry and task loads.

If the generalized errors, ε, can be found from calibration measurements, then the correct end-effector position and orientation error can be calculated and compensated for using Eq. (3). Fig. 5 schematically shows an error compensation algorithm based on Eq. (3).

The method to obtain ε from experimental measurements is to measure components of vector $\Delta\mathbf{X}$ at m different configurations, defined as $\mathbf{q_1}, \mathbf{q_2}, \ldots, \mathbf{q_m}$, resulting in:

$$\Delta\mathbf{X_t} = \begin{bmatrix} \Delta\mathbf{X_1} \\ \Delta\mathbf{X_2} \\ \ldots \\ \Delta\mathbf{X_m} \end{bmatrix} = \begin{bmatrix} \mathbf{J_e(q_1)} \\ \mathbf{J_e(q_2)} \\ \ldots \\ \mathbf{J_e(q_m)} \end{bmatrix} \cdot \varepsilon = \mathbf{J_t} \cdot \varepsilon \tag{4}$$

To compensate for the effects of measurement noise, the number of measurements m is, in general, much larger than n.
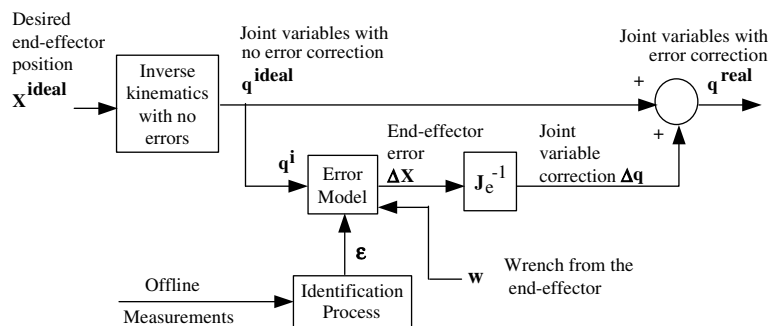

Fig. 5. Error compensation scheme.

If the generalized errors ε are constant, then a unique least-squares estimate $\hat{\varepsilon}$ can be calculated by:

$$\hat{\varepsilon} = \left(\mathbf{J_t^T J_t}\right)^{-1} \mathbf{J_t^T} \cdot \Delta \mathbf{X_t} \tag{5}$$

However, if the identification Jacobian matrix $\mathbf{J_e(q_i)}$ contains linearly dependent columns, Eq. (5) will produce estimates with poor accuracy [8]. This occurs when there is redundancy in the error model, in which case it is not possible to distinguish the error contributed by each generalized error component. Orthogonal matrix decomposition can be used in these cases to improve the numerical accuracy of this approach. Analytical procedures can also be employed to eliminate these redundant parameters [25].

On the other hand, if non-geometric factors are considered such as link compliance or gear eccentricity, then it is necessary to represent the parameters of ε as a function of the system configuration and task loadings prior to the identification process. This extended modeling is presented below.

3. Geometric and elastic error compensation

In this section, elastic deformation and classical geometric errors are considered in a unified manner. The error model must be extended to consider the task loading wrench and configuration dependency of the errors. For a system with significant geometric and elastic errors, the generalized errors ε are a function of the manipulator configuration $\mathbf{q}$ and the end-effector wrench $\mathbf{w}$, namely $\varepsilon(\mathbf{q}, \mathbf{w})$. To predict the endpoint position of the manipulator for a given configuration and task wrench, it is necessary to calculate the generalized errors from a set of offline measurements. The complexity of these calculations can be substantially reduced if the generalized errors are parameterized using polynomial functions. Here, the ith element of vector ε is approximated by a polynomial series expansion of the form:

$$\varepsilon_i = \sum_{j=1}^{n_i} c_{i,j} \cdot f_{i,j}(\mathbf{q}, \mathbf{w}), \quad f_{i,j}(\mathbf{q}, \mathbf{w}) \equiv (w_{m_j})^{a_{0,j}} \cdot \left(q_1^{a_{1,j}} \cdot q_2^{a_{2,j}} \cdot \ldots \cdot q_n^{a_{n,j}}\right) \tag{6}$$

where n_i is the number of terms used in each expansion, $c_{i,j}$ are the polynomial coefficients, w_{mj} is an element of the task wrench $\mathbf{w}$, and $q_1, q_2, \ldots, q_n$ are the manipulator joint parameters. It has been found that good accuracy can be obtained using only a few terms n_i in the above expansion [26]. From the definition of the generalized errors, the errors associated with the ith link depend only on the parameters of the ith joint. If elastic deflections of link i are considered, then the generalized errors created by these deflections would depend on the weight wrench w_i applied at the ith link. For a serial manipulator, this wrench is due to the wrench at the end-effector and to the configuration of the links after the ith. Hence, the wrench w_i depends only on the joint parameters $q_{i+1}, \ldots, q_n$. Thus, the number of terms in the products of Eq. (6) is substantially reduced. Each generalized error parameter is then represented as a function of only a few of the system variables, greatly reducing the number of measurements required to characterize the system using the GEC method. In addition, if only simple (linear elastic) beam bending is considered, then the polynomial order can be reduced to three relating the joint parameters and one relating the payload

wrench. Higher order terms may be needed to model geometric errors of prismatic joints, such as rail curvature, discussed in the next section.

The constant coefficients $c_{i,j}$ are then grouped into one vector **c**, becoming the unknowns of the problem. Once the polynomial coefficients, **c**, are identified, the end-effector position and orientation error $\Delta \mathbf{X}$ can be calculated and compensated using Eqs. (3) and (6). Note that all redundant parameters are eliminated prior to the model expansion. If redundant parameters are introduced after the error model expansion (which can be verified from the condition number of the pseudo-inverse of the Identification Jacobian), then classical numerical methods can be applied to eliminate them.

An advantage of the polynomial approximation is the modeling of non-linear elasticity, through terms with order higher than three, as well as considering a general formulation for geometric errors that are allowed to vary in their own frames such as in the case of rail curvature. In the next section, the geometric and elastic compensation method is applied to the patient positioning system.

4. Application to the patient positioning system

The PPS is a six degree of freedom robot manipulator (see Fig. 2) built by General Atomics [2]. The first three joints are prismatic, with maximum travel of 225 cm, 56 cm and 147 cm for the lateral (X), vertical (Y) and longitudinal (Z) axes, respectively. The last three joints are revolute joints. The first joint rotates parallel to the vertical (Y) axis and can rotate $\pm 90°$. The last two joints are used for small corrections around an axis of rotation parallel to the Z (roll) and X (pitch) axes, and have a maximum rotation angle of $\pm 3°$. The manipulator end-effector is a couch, supporting the patient in a supine position, accommodating patients up to 188 cm in height and 300 lbs in weight in normal operation.

The intersection point of the proton beam with the gantry axis of rotation is called the system isocenter. The treatment volume is defined by a treatment area on the couch of 50 cm × 50 cm and a height of 40 cm (see Fig. 2). This area covers all possible locations of treatment points (i.e. tumor locations at a patient). The objective is that the PPS makes any point in this volume be coincident with the isocenter at any orientation.

The joint parameters of the PPS are the displacements d_1, d_2, d_3 of the three prismatic joints and the rotations θ, α, β of the three rotational joints. A 6-axis force/torque sensor is placed between the couch and the last joint. By measuring the forces and moment at this point, it is possible to calculate the patient weight and the coordinates of the patient center of gravity. The system motions are very slow and smooth due to safety requirements. Hence, the system is quasi-static, and its dynamics do not influence the system accuracy and are neglected.

The accuracy of the PPS was measured using a Leica 3D Laser Tracking System. These measurements were to evaluate the PPS repeatability, the nonlinearity of its weight dependent deflections, the inherent uncompensated PPS accuracy, and the method discussed in the previous section.

Three targets were placed on the couch at the positions P_1, P_2 and P_3, shown in Fig. 6. The targets are located about 10 mm above the couch. The position accuracy of the measurements is approximately 0.04 mm.
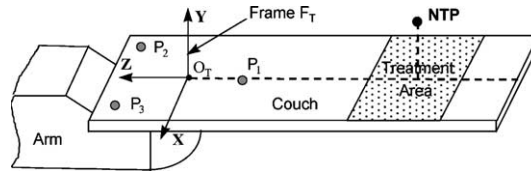
Fig. 6. Close view of the PPS couch.

A reference frame F_T is fixed to the couch (see Fig. 6). The intersection point of the plane $(P_1P_2P_3)$ with the Y axis of the fixed reference frame is called O_T. A fixed reference frame, F_0, is used to express the coordinates of all points. When the PPS is at its home configuration (all joint variables set equal to zero) the reference frames F_T and F_0 are coincident. The location of a tumor on a patient, defined as the Nominal Treatment Point (NTP), is specified in the frame coordinate F_T. For the results presented below, the NTP coordinates in F_T are taken as $(0, 90, -840)$ mm.

From separate measurements of the couch compliance, it has been found that significantly larger elastic deformations (compared to the deformations of the rest of the system) are associated with the couch. In order not to compromise the system calibration accuracy due to numerical errors caused by such different magnitudes (i.e., numerical error propagation due to bad scaling), the measurement points were carefully chosen not to include the couch compliance, see Fig. 6. This is the reason why the targets were placed near the manipulator wrist, away from the Nominal Treatment Point. Thus, the couch has been considered to be outside the robot model, and its parameters were not included in the formulation. Separate measurements have been conducted by General Atomics to identify the couch compliance, and the associated elastic deformations (to be later included in the complete model, out of the scope of this work). This procedure allows for a better identification of the Patient Positioning System parameters, while allowing couch replacing without the need for recalibrating the entire system.

For more than 700 different configurations of the PPS and different weights, the location of points P_1, P_2 and P_3 in frame F_0 were measured and the NTP coordinates in frame F_0 calculated. From the system kinematic model with no errors, the ideal coordinates of NTP were calculated and subtracted from the experimentally measured values to yield the vector $\Delta \mathbf{X}(\mathbf{q},\mathbf{w})$. Four hundred and fifty measurements were used to evaluate the basic uncompensated accuracy of the PPS and the accuracy of the compensation method described above. Two different payloads were used: one with no weight and another with a 154 lb weight at the center of the treatment area. The PPS configurations used were grouped into two sets:

Set (a) *Treatment volume*. The eight vertices of the treatment volume (see Fig. 2) are reached with the NTP with angle θ taking values from $-90°$ to $90°$ with a step of $30°$, for a total of 112 configurations.

Set (b) *Independent motion of each axis*. Each axis is moved independently while all other axes are held at the home (zero) values. The step of motion for d_1 is 50 mm, for d_2 20 mm, for d_3 25 mm and for θ 5°, resulting in 338 configurations.

The PPS uncompensated accuracy combining the two sets is shown in Fig. 7. The data points represent the positioning errors of NTP. It is clearly seen that in spite of the high quality of the
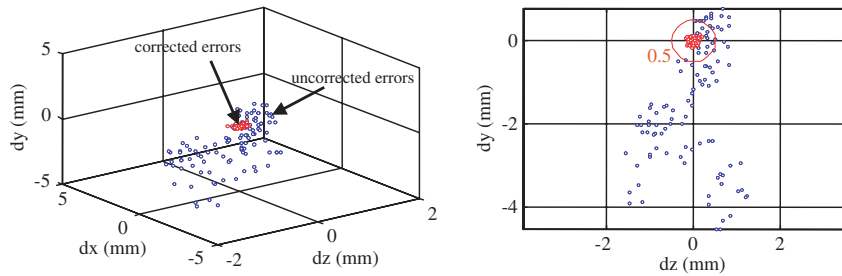
Fig. 7. Measured and residual errors after compensation.

PPS physical system, its uncompensated accuracy is on the order of 10 mm. This is approximately 20 times higher than the specification of ±0.50 mm.

Part of the uncompensated error is the repeatability errors. These errors are due to the random system errors, and they cannot be compensated by the calibration method. They represent the accuracy limit of any error compensation algorithm and they also show how well an error compensation technique performs. Here the system repeatability is based on how well the system would return to the NTP from certain arbitrary configurations. A total of 270 measurements were taken with zero payload weight. The repeatability error of the PPS is less than 0.15 mm (3σ). Thus this system is a good candidate for model based error correction methods, since the repeatability errors are relatively small compared to the ±0.50 mm.

In implementing the computation method, a general nonlinear function of the wrench **w** can be used. To help establish this function, the behavior of the PPS positioning errors for different payload weights was examined with measurements made at the home (zero) configuration. The weights ranged from 0 to 300 lbs in steps of approximately 25 lbs. The results showed that the positioning errors of the PPS were nearly linear with the payload weight. The least square error is less than 0.1 mm for the linear fit. Hence, the generalized errors were taken as linear functions of the system wrench in Eq. (6).

The redundant error parameters are then eliminated from the error model. After the model expansion to include elastic deformations, one redundant parameter is introduced due to the polynomial representation of the errors. This remaining redundant parameter is easily removed using classical numerical methods [8]. The generalized errors are then calculated with Eq. (6) using the configurations of set (b) (independent motion of its axes) and half of the treatment volume data (set a). For a Pentium PC 300 MHz, the computing time was less than one minute. The PPS is then commanded to go to compensated points for the remaining configurations of set (a). The residual positioning errors of the PPS after compensation for these points are shown in Fig. 7. The residual errors are enclosed in a sphere of 0.38 mm radius, which is smaller than the sphere of 0.5 mm radius that represents the accuracy specification. The required number of data points for this calculation was less than 400. The error distribution along each axis is shown in Fig. 8. Hence the compensation method used in this paper enables the system to meet its specification. It is now a key element in MGH's operational software. Since the remaining errors after calibration using 400 points were comfortably under 0.5 mm, a significantly smaller number of poses could have been used in the calibration. In fact, applying the presented calibration method to a subset of only 125 measurement poses of the patient positioning system resulted in a maximum residual error of
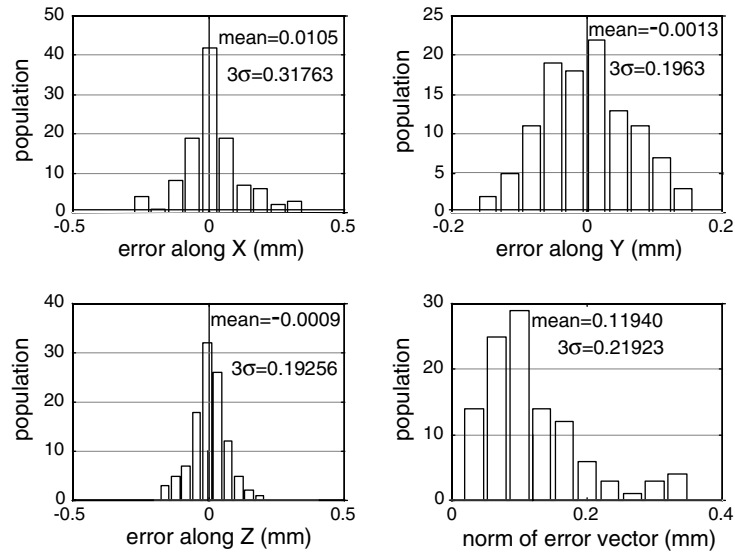
Fig. 8. The statistics of the compensated PPS errors at NTP.

0.49 mm. This absolute accuracy meets the specification, while significantly less than 400 measurement points would be necessary. This number is indeed much smaller than it might be expected, considering that not only elastic deformations, but also geometric errors that vary in their own frames (such as a quasi-sinusoidal shape for the rail errors on the prismatic base, as discussed below) are present in the system.

One of the main advantages of the polynomial approach is the ability to model non-linearities or any other repeatable error source that can be represented as a function of the system parameters and of the payload wrenches. In particular, the errors along the Patient Positioner's lateral rail had an approximately sinusoidal shape (as it was expected from the respective manufacturing process, due to eccentricities in its machining), which turned out to be an important error source in this system. These errors were identified through the presented methodology using polynomial expansions with relatively few terms (about eighth order).

Note also that the polynomial modeling automatically accounts for the elastic deformations due to link masses. The polynomial terms that are a function of the system configuration (but not of the task wrench **w**) are the ones that account for the contribution of the link masses to the varying end-effector elastic errors. Since the link masses are constant, the constant polynomial coefficients associated with these terms will automatically account for such configuration-dependent effects. Therefore, all link masses are implicitly identified, and their associated elastic errors are automatically compensated for.

5. Summary and conclusions

In this work, a high-accuracy large medical manipulator was calibrated, compensating for the positioning end-effector errors under significant task loads. Both geometric and elastic deforma-

tion errors were considered using polynomial approximations. The results showed that the basic accuracy of the manipulator exceeded its specifications, but after applying the method to compensate for end-effector errors the accuracy specifications were met. The error compensation routines are now a key element of the patient positioning system software used to treat cancer patients.

Acknowledgement

References

[1] C. Vaillancourt, G. Gosselin, 1994. Compensating for the structural flexibility of the SSRMS with the SPDM, in: Proceedings of the International Advanced Robotics Program, Second Workshop on Robotics in Space, Canadian Space Agency, Montreal, Canada.

[2] J. Flanz, et al., 1996. Design approach for a highly accurate patient positioning system for NPTC, in: Proceedings of the PTOOG XXV and Hadrontherapy Symposium, Belgium, pp. 1–5.

[3] W. Hamel, S. Marland, T. Widner, 1997. A model-based concept for telerobotic control of decontamination and dismantlement tasks, in: Proceedings of the 1997 IEEE International Conference of Robotics and Automation, Albuquerque, New Mexico.

[4] P. Drouet, S. Dubowsky, C. Mavroidis, 1998. Compensation of geometric and elastic deflection errors in large manipulators based on experimental measurements: application to a high accuracy medical manipulator, in: Proceedings of the 6th International Symposium on Advances in Robot Kinematics, Austria, pp. 513–522.

[5] P. Drouet, 1999. Modeling, identification and compensation of positioning errors in high accuracy manipulators under variable loading: application to a medical patient positioning system, Ph.D. Thesis, Université de Poitiers, France.

[6] Z.S. Roth, B.W. Mooring, B. Ravani, 1986. An overview of robot calibration, in: IEEE Southcon Conference, Orlando, Florida, pp. 377–384.

[7] J. Hollerbach, A survey of kinematic calibration, in: O. Khatib, et al. (Eds.), Robotics review, MIT Press, Cambridge MA, 1988.

[8] J.M. Hollerbach, C.W. Wampler, The calibration index and taxonomy for robot kinematic calibration methods, International Journal of Robotics Research 15 (6) (1996) 573–591.

[9] H. Zhuang, J. Wu, W. Huang, 1996. Optimal planning of robot calibration experiments by genetic algorithms, in: Proceedings of IEEE 1996 International Conference on Robotics and Automation, Minneapolis, pp. 981–986.

[10] K. Waldron, V. Kumar, 1979. Development of a theory of errors for manipulators, in: Proceedings of the Fifth World Congress on the Theory of Machines and Mechanisms, pp. 821–826.

[11] C. Wu, A kinematic CAD tool for the design and control of a robot manipulator, International Journal of Robotics Research 3 (1) (1984) 58–67.

[12] R. Vaichav, E. Magrab, A general procedure to evaluate robot positioning errors, International Journal of Robotics Research 6 (1) (1987) 59–74.

[13] C. Mirman, K. Gupta, Identification of position independent robot parameter errors using special Jacobian matrices, International Journal of Robotics Research 12 (3) (1993) 288–298.

[14] P. Broderick, R. Cirpa, A method for determining and correcting robot position and orientation errors due to manufacturing, Transactions of the ASME, Journal of Mechanisms, Transmissions and Automation in Design 110 (1988) 3–10.

[15] H. Zhuang, Z. Roth, F. Hamano, A complete and parametrically continuous kinematic model for robot manipulators, IEEE Transaction in Robotics and Automation 8 (4) (1992) 451–462.

[16] J.H. Borm, C.H. Menq, Determination of optimal measurement configurations for robot calibration based on observability measure, International Journal of Robotics Research 10 (1) (1991) 51–63.

[17] S. Dubowsky, J. Maatuk, N.D. Perreira, A parametric identification study of kinematic errors in planar mechanisms, Transactions of ASME Journal of Engineering for Industry 1 (1975) 635–642.

[18] H. Zhuang, Z.S. Roth, 1993. A linear solution to the kinematic parameter identification of robot manipulators, IEEE Transactions in Robotics and Automation 9 (2) (1993) 174–185.

[19] J. Flanz, et al., Overview of the mgh-northeast proton therapy center: plans and progress, Nuclear Instruments and Methods in Physics Research B 99 (1995) 830–834.

[20] I. Rabinowitz, Accuracy of radiation field alignment in clinical practice, International Journal of Radiation Oncology Biology and Physics 11 (1985) 1857–1867.

[21] C. Mavroidis, S. Dubowsky, P. Drouet, J. Hintersteiner, J. Flanz, 1997. A systematic error analysis of robotic manipulators: application to a high performance medical robot, in: Proceedings of the 1997 IEEE Int. Conference of Robotics and Automation, Albuquerque, New Mexico, pp. 980–985.

[22] A. Slocum, Precision Machine Design, Englewood Cliffs, 1992.

[23] J. Craig, Introduction to Robotics: Mechanics and Control, Addison-Willey, 1989.

[24] H. Zhuang, S.H. Motaghedi, Z.S. Roth, 1999. Robot calibration with planar constraints, in: Proceedings of the IEEE International Conference of Robotics and Automation, Detroit, Michigan, pp.805–810.

[25] M. Meggiolaro, S. Dubowsky, 2000. An analytical method to eliminate the redundant parameters in robot calibration, in: Proceedings of the International Conference on Robotics and Automation (ICRA '2000), IEEE, San Francisco, pp. 3609–3615.

[26] M. Meggiolaro, C. Mavroidis, S. Dubowsky, 1998. Identification and compensation of geometric and elastic errors in large manipulators: application to a high accuracy medical robot, in: Proceedings of the 25th Biennial Mechanisms Conference, ASME, Atlanta.